SUPPLEMENTARY METHODS

Study Design

This study included patients ≥ 21 years old with stage 5 CKD/ESKD and scheduled for AVF creation at Jackson Memorial Hospital and the University of Miami Hospital. A single surgeon (M.T.) performed all surgical procedures and preoperative vascular mapping of the upper extremities to plan the AVF.[S1] We followed the order of AVF preference recommended by the National Kidney Foundation/Kidney Disease Outcomes Quality Initiative.[S2] The surgeon collected vascular samples of the pre-access vein used to create the arteriovenous anastomosis and/or the juxta-anastomotic area of the AVF during second-stage AVF creation if the length of the transected AVF was long enough to allow its transposition.

Tissue pairs (veins and AVFs) were collected from 60 participants from November 2014 to November 2018 as part of an actively enrolling biorepository. These included 30 patients with successful AVF maturation and 30 with maturation failure (**Figure 1B**). Patients were selected from the repository such that both groups had similar representation of baseline characteristics (age range, sex distribution, ethnicity, comorbidities, previous vascular access history), and did not meet the following exclusion criteria: 1) proximal brachial-brachial AVF for planned graft extension, 2) intravascular intervention prior to second-stage surgery, 3) primary access thrombosis, 4) steal syndrome, and 5) active infection during AVF maturation. Inclusion criteria for bulk RNA sequencing consisted of an RNA Integrity Score [RIN]>5 in both the pre-access vein and AVF sample from each pair. Using this criterion, a total of 38 tissue pairs (19 patients from each group) were submitted for pairwise RNA-seq analysis (**Figure 1B**).

Anatomic AVF non-maturation was defined retrospectively as an AVF that never achieved a luminal diameter ≥ 6 mm, and which required a shorter transposition, graft extension, or ligation instead of the standard transposition during second-stage surgery.[S1] The anatomic maturation definition is a simplified version of the "rule of sixes", specifically suited to evaluate the biology of early vascular remodeling when cannulation-related confounders have not played a role. The study was performed according to the ethical principles of the Declaration of Helsinki and regulatory requirements at both institutions. The ethics committee and Institutional Review Board at the University of Miami approved the study.

Surgical Technique

Patients underwent venous and arterial mapping of the upper extremities using Duplex ultrasound. As per our protocol, we used the most peripheral vein that was ≥ 3.5 mm, the brachial artery if ≥ 4.0 mm or the radial artery if ≥ 2.5 mm. All procedures involved monitored anesthesia care (MAC). The basilic vein or brachial vein was located and transected above the elbow. The first vein biopsy was collected at this time. The vein was flushed with heparinized saline and the entire length of a coronary dilator (Teleflex, Morrisville, NC) was passed to make sure there was no obstruction. The size of the dilator was noted as the diameter of the vein.

An end vein-to-side artery anastomosis was performed using the standard running parachute technique. The surgeon dissects and ties off the basilic vein entering the arm from the forearm and the medial cubital vein above the elbow. The basilic vein proximal to the above branches or to any large branch was used in order to force all the flow into that vein and avoid any shunting into the branch. The median anastomosis diameter was 4.5 mm [IQR 4.5-5.0]. The incision was closed only if the radial pulse was maintained and the thrill was easily palpable

through the skin. Immediately after anastomosis, the vein was compressed as proximal as possible in the upper arm allowing the increased pressure in the vein to dilate it. If the radial pulse was not palpable, banding of the inflow segment of the vein was performed with either clips or sutures to decrease the caliber to a diameter similar to the artery.

All two-stage AVF patients included in the study underwent the second-stage procedure. The median time for the second stage surgery was 74 days [IQR 63 – 98]. We evaluated the first stage procedure by physical exam and Duplex ultrasound using tourniquet. The transposition was done by transecting the AVF, routing it subcutaneously and then re-anastomosing to the stump on the artery or a new more proximal anastomosis was done. Care was taken not to create the tunnel too lateral in order to avoid a large angle in the proximal arm. If a significant portion of the AVF was < 6 mm in diameter, then a graft extension was done to the more proximal dilated vein. If the vein was too short, a new anastomosis was done to the brachial artery proximal to the ligated stump.

Specimen Collection and Tissue Processing

Native vein and AVF venous samples, 1-5 mm in length, were submerged in RNA*later* (QIAGEN, Germantown, MD) immediately after collection, de-identified with a numerical code, and stored at -80˚C. If enough tissue was available, a 1-2 mm cross-section was fixed in 10% neutral formalin (Sigma-Aldrich, St. Louis, MO) before paraffin embedding and sectioning.

A 1-mm cross-section (~50-60 mg of tissue) was ground to a fine powder in a Spex/Mill 6770 cryogenic grinder (SPEX SamplePrep, Metuchen, NJ). Total RNA was isolated with Trizol (Thermo Fisher Scientific, Waltham, MA) and further purified using the E.Z.N.A. Total RNA Kit I (Omega Bio-tek, Norcross, GA) as previously described.[S3] For whole cell protein isolation,

ground powder from similar-sized tissues was resuspended in protein extraction buffer as previously described.[S3]

RNA Sequencing and Bioinformatic Analyses

Preparation and sequencing of RNA libraries was carried out in the John P. Hussman Institute for Human Genomics, Center for Genome Technology. Briefly, total RNA was quantified and qualified using the Agilent Bioanalyzer to have an RNA Integrity Score (RIN)>5. 500 ng of total RNA was used as input for the Illumina TruSeq Stranded Total RNA Library Prep Kit with Ribo-Zero to create ribosomal RNA-depleted sequencing libraries. Each sample had a unique barcode to allow for multiplexing and was sequenced to >40 million raw reads in a single end 75bp sequencing run on the Illumina NextSeq500. Raw sequence data was processed by the on-instrument Real Time Analysis software (v.2.4.11) to basecall files. These were converted to de-multiplexed FASTQ files with the Illumina supplied scripts in the BCL2FASTQ software (v2.17). The quality of the reads was determined with the FASTQC software (http://www.bioinformatics.babraham.ac.uk/projects/fastqc/) to evaluate per base sequence quality, duplication rates, and overrepresented k-mers. Illumina adapters were trimmed from the ends of the reads using the Trim Galore! package (http://www.bioinformatics.babraham.ac.uk/projects/trim_galore/). Reads were aligned to the human reference genome (hg38) with the STAR aligner (v2.5.2).[S4] Gene count quantification for total RNA was performed using the GeneCounts function within STAR against the GENCODE v25 human transcript .gtf file.

Differential expressed genes (DEGs) between pre-access veins and AVFs were identified in DESeq2[S5] using a paired algorithm accounting for the time of tissue collection (vein *vs.* AVF)

and the patient origin of each set of paired samples (design= ~Subject + time). Changes in gene expression during the vein to AVF transformation in relation to maturation failure were further detected by conditioning the above analyses to differences between outcomes (design= ~Subject + time * outcome). This multifactorial analysis evaluates the interaction between time (postoperative change) and outcome, as explained in detail in the Bioconductor support site (DESEq2 Paired samples Before and after treatment (bioconductor.org)). The false discovery rate (FDR) was determined by applying the Benjamini-Hochberg multiplicity correction method. Gene set enrichment analyses (GSEA) of DEGs (absolute $\log_2$FC ≥ 1, FDR <0.05) were performed using the package clusterProfiler.[S6] Similarly, to predict transcription factors regulating DEGs, highly expressed DEGs (baseMean>50) were used as the input gene set in the ChEA3 transcription factor enrichment analysis (TFEA).[S7] Information about gene functions was obtained from QIAGEN Ingenuity Pathway Analysis.[S8] Classification of genes as part of the "matrisome" was based on the MatrisomeDB annotation database[S9] and a summary of proteoglycan biosynthetic/modifying enzymes previously published.[S10] The raw RNA-seq data are accessible in NCBI Gene Expression Omnibus through the GEO accession numbers GSE119296 and GSE220796.

Cytokine Multiplex Assays

Tissue protein lysates of vein and AVF pairs were normalized to 400 µg/mL and profiled using the Human Cytokine/Chemokine 48-Plex Discovery Assay (catalog no. HD48) and the TGFβ 3-Plex Discovery Assay (catalog no. TGFB1-3) by Eve Technologies Corporation (Calgary, AB, Canada). For the purposes of statistical analysis, values below the quantification limit (QL) were assigned the minimum value of QL.

Histology and Immunohistochemistry Analyses

Vein and AVF tissue sections were stained with Masson's trichrome (Polysciences, catalog #25088-1) and Alcian blue (Abcam, #ab150662) for gross histomorphometric analysis. Medial fibrosis (% area of collagen), IH (defined as the intima/media area ratio), and proteoglycan content in the intima (% area) were quantified using ImageJ (National Institutes of Health) and color thresholding methods. Operators blinded to the clinical data performed image digital processing and morphometric measurements.

For IHC, paraffin sections were rehydrated by serially immersing them in xylene, alcohol, and water, and antigens retrieved by boiling slides in 10 mM citrate buffer, pH 6.0 for 20 minutes, except for collagen III, which required proteinase K incubation for 10 minutes for antigen retrieval. Sections were incubated with Dako Peroxidase Blocking Solution (#K4005) for 10 min, followed by Dako Protein Blocking Solution (#X0909) for 1 hour. Specific proteins were detected by incubating overnight at 4°C with the following primary antibodies: collagen III (Thermo Fisher, #22734-1-AP, 1:3500), collagen VIII (Abcam, #ab236653, 1:1000), aggrecan (Thermo Fisher, #13880-1-AP, 1:100), versican (Thermo Fisher, #MA5-34654, 1:100), IL-6 (Novus Biologicals, #NB600-1131, 1:500), and osteopontin (Thermo Fisher, #25715-1-AP, 1:50). Bound antibodies were detected using the Dako Universal Link kit (Agilent, Santa Clara, CA), and color was developed with the Dako DAB+ Substrate Chromogen System (Agilent). Nuclei were counterstained with Meyer's hematoxylin and mounted in Entellan mounting medium (Sigma-Aldrich). Images were acquired using a VisionTek DM01 digital microscope (Sakura Finetek, Torrance, CA).

Statistical Analysis

Statistical analyses of morphometry and protein validation data were performed using GraphPad Prism 8.4.0 (San Diego, CA). Normally distributed data were compared using t-tests and expressed as mean ± standard deviation (SD) or mean ± standard error of the mean (SEM) where indicated. If normality assumptions were not met, the Mann-Whitney test was used, and data expressed as median and interquartile range (IQR). Vein-to-AVF comparisons of morphometry and protein levels were performed using paired t-tests or paired Wilcoxon signed-rank tests as appropriate.

REFERENCES

S1. Tabbara M, Duque JC, Martinez L, Escobar LA, Wu W, Pan Y, Fernandez N, Velazquez OC, Jaimes EA, Salman LH, et al. Pre-existing and Postoperative Intimal Hyperplasia and Arteriovenous Fistula Outcomes. *Am J Kidney Dis*. 2016;68:455-464. doi: 10.1053/j.ajkd.2016.02.044

S2. Lok CE, Huber TS, Lee T, Shenoy S, Yevzlin AS, Abreo K, Allon M, Asif A, Astor BC, Glickman MH, et al. KDOQI Clinical Practice Guideline for Vascular Access: 2019 Update. *Am J Kidney Dis*. 2020;75:S1-S164. doi: 10.1053/j.ajkd.2019.12.001

S3. Martinez L, Tabbara M, Duque JC, Selman G, Falcon NS, Paez A, Griswold AJ, Ramos-Echazabal G, Hernandez DR, Velazquez OC, et al. Transcriptomics of Human Arteriovenous Fistula Failure: Genes Associated With Nonmaturation. *Am J Kidney Dis*. 2019;74:73-81. doi: 10.1053/j.ajkd.2018.12.035

S4. Dobin A, Davis CA, Schlesinger F, Drenkow J, Zaleski C, Jha S, Batut P, Chaisson M, Gingeras TR. STAR: ultrafast universal RNA-seq aligner. *Bioinformatics*. 2013;29:15-21. doi: 10.1093/bioinformatics/bts635

S5. Love MI, Huber W, Anders S. Moderated estimation of fold change and dispersion for RNA-seq data with DESeq2. *Genome Biol*. 2014;15:550. doi: 10.1186/s13059-014-0550-8

S6. Wu T, Hu E, Xu S, Chen M, Guo P, Dai Z, Feng T, Zhou L, Tang W, Zhan L, et al. clusterProfiler 4.0: A universal enrichment tool for interpreting omics data. *Innovation (Camb)*. 2021;2:100141. doi: 10.1016/j.xinn.2021.100141

S7. Keenan AB, Torre D, Lachmann A, Leong AK, Wojciechowicz ML, Utti V, Jagodnik KM, Kropiwnicki E, Wang Z, Ma'ayan A. ChEA3: transcription factor enrichment analysis by orthogonal omics integration. *Nucleic Acids Res*. 2019;47:W212-W224. doi: 10.1093/nar/gkz446

S8. QIAGEN IPA; QIAGEN Inc., https://digitalinsights.qiagen.com/IPA; Accessed 11/02/2021.

S9. Shao X, Taha IN, Clauser KR, Gao YT, Naba A. MatrisomeDB: the ECM-protein knowledge database. *Nucleic Acids Res*. 2020;48:D1136-D1144. doi: 10.1093/nar/gkz849

S10. Gottschalk J, Elling L. Current state on the enzymatic synthesis of glycosaminoglycans. *Curr Opin Chem Biol*. 2021;61:71-80. doi: 10.1016/j.cbpa.2020.09.008

Supplementary Table S1. Accession numbers of raw sequencing data in the NCBI Gene Expression Omnibus repository

Patient No. (Samples)	Age	Sex	Race / Ethnicity	Outcome	Vein	AVF
1 (V006, T032)	44	M	Black	Matured	GSE119296	GSE119296
2 (V012, T024)	51	M	White	Matured	GSE119296	GSE119296
4 (V035, T052)	81	M	Hispanic	Matured	GSE119296	GSE119296
5 (V063, T072)	80	M	White	Matured	GSE119296	GSE119296
6 (V167, T362)	66	M	Black	Matured	GSE119296	GSE119296
7 (V066, T093)	23	F	Hispanic	Matured	GSE119296	GSE119296
8 (V155, T171)	67	F	Black	Matured	GSE119296	GSE119296
9 (V385, T382)	42	F	Black	Matured	GSE119296	GSE119296
10 (V390, T394)	60	F	White	Matured	GSE119296	GSE119296
11 (V399, T390)	65	F	Hispanic	Matured	GSE119296	GSE119296
12 (V056, T073)	50	M	Hispanic	Failed	GSE119296	GSE119296
13 (V165, T372)	84	M	Hispanic	Failed	GSE119296	GSE119296
14 (V401, T389)	40	M	Black	Failed	GSE119296	GSE119296
15 (V011, T027)	67	F	White	Failed	GSE119296	GSE119296
16 (V013, T036)	62	F	Black	Failed	GSE119296	GSE119296
17 (V034, T054)	80	F	Black	Failed	GSE119296	GSE220796
18 (V058, T071)	58	F	Black	Failed	GSE119296	GSE119296
19 (V062, T076)	59	F	Hispanic	Failed	GSE119296	GSE119296
22 (V176, T370)	43	M	Hispanic	Matured	GSE220796	GSE220796
23 (V431, T420)	33	M	Black	Matured	GSE220796	GSE220796
24 (V462, T436)	48	M	Black	Matured	GSE220796	GSE220796
25 (V475, T438)	39	M	Hispanic	Matured	GSE220796	GSE220796
26 (V413, T402)	68	F	Black	Matured	GSE220796	GSE220796
27 (V445, T413)	45	F	Black	Matured	GSE220796	GSE220796
28 (V460, T424)	32	F	Black	Matured	GSE220796	GSE220796
29 (V469, T433)	64	F	White	Matured	GSE220796	GSE220796
30 (V522, T474)	75	F	Hispanic	Matured	GSE220796	GSE220796
31 (V501, T462)	38	M	Hispanic	Failed	GSE220796	GSE220796
32 (V519, T480)	67	M	Hispanic	Failed	GSE220796	GSE220796
33 (V523, T472)	67	M	Hispanic	Failed	GSE220796	GSE220796
34 (V532, T484)	48	M	Black	Failed	GSE220796	GSE220796
35 (V487, T452)	68	M	Black	Failed	GSE220796	GSE220796
36 (V496, T453)	40	M	Black	Failed	GSE220796	GSE220796
37 (V497, T455)	60	M	Black	Failed	GSE220796	GSE220796
38 (V439, T414)	74	F	White	Failed	GSE220796	GSE220796
39 (V467, T432)	64	F	Black	Failed	GSE220796	GSE220796
40 (V471, T453B)	47	F	Hispanic	Failed	GSE220796	GSE220796
41 (V530, T483)	46	F	Black	Failed	GSE220796	GSE220796

Patients 3, 20, and 21 had incomplete tissue pairs in GSE119296.

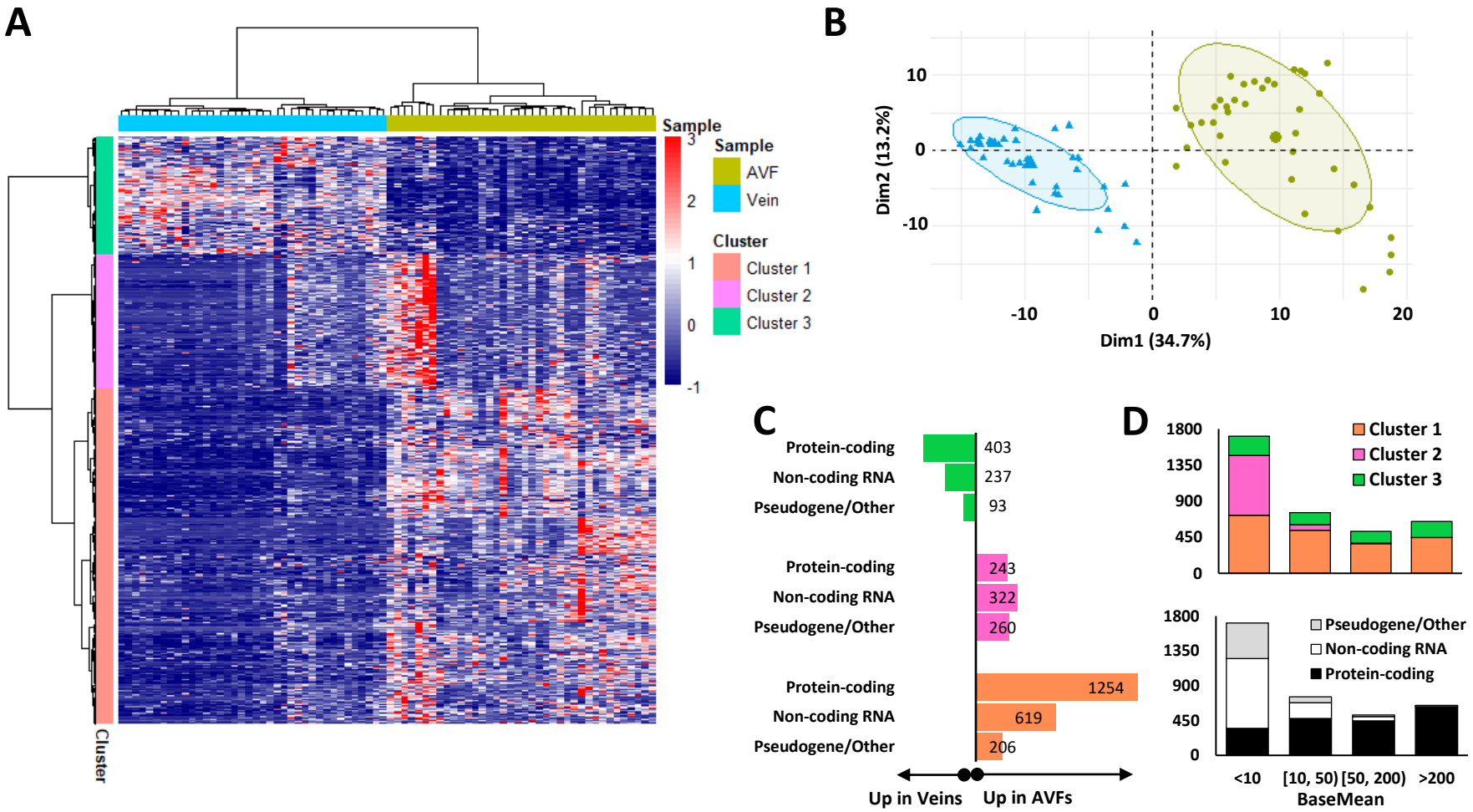

Supplementary Figure S1. Summary of transcriptomic changes during the vein to AVF transformation. A) Heatmap of 3,637 differentially expressed genes (absolute log2FC ≥ 1; FDR<0.05) between 38 pre-access veins and their corresponding AVFs. **B)** Principal component analysis of vein (blue) and AVF samples (green) based on gene expression differences. **C)** Distribution of gene biotypes per cluster identified in panel A. Bars indicate the number of genes per biotype category. **D)** Distribution of clusters and biotypes according to normalized expression levels (baseMean). Expression cutoffs of <10, [10-50), [50-200), and >200 indicate genes with low, moderately low, moderately high, and high expression levels, respectively.

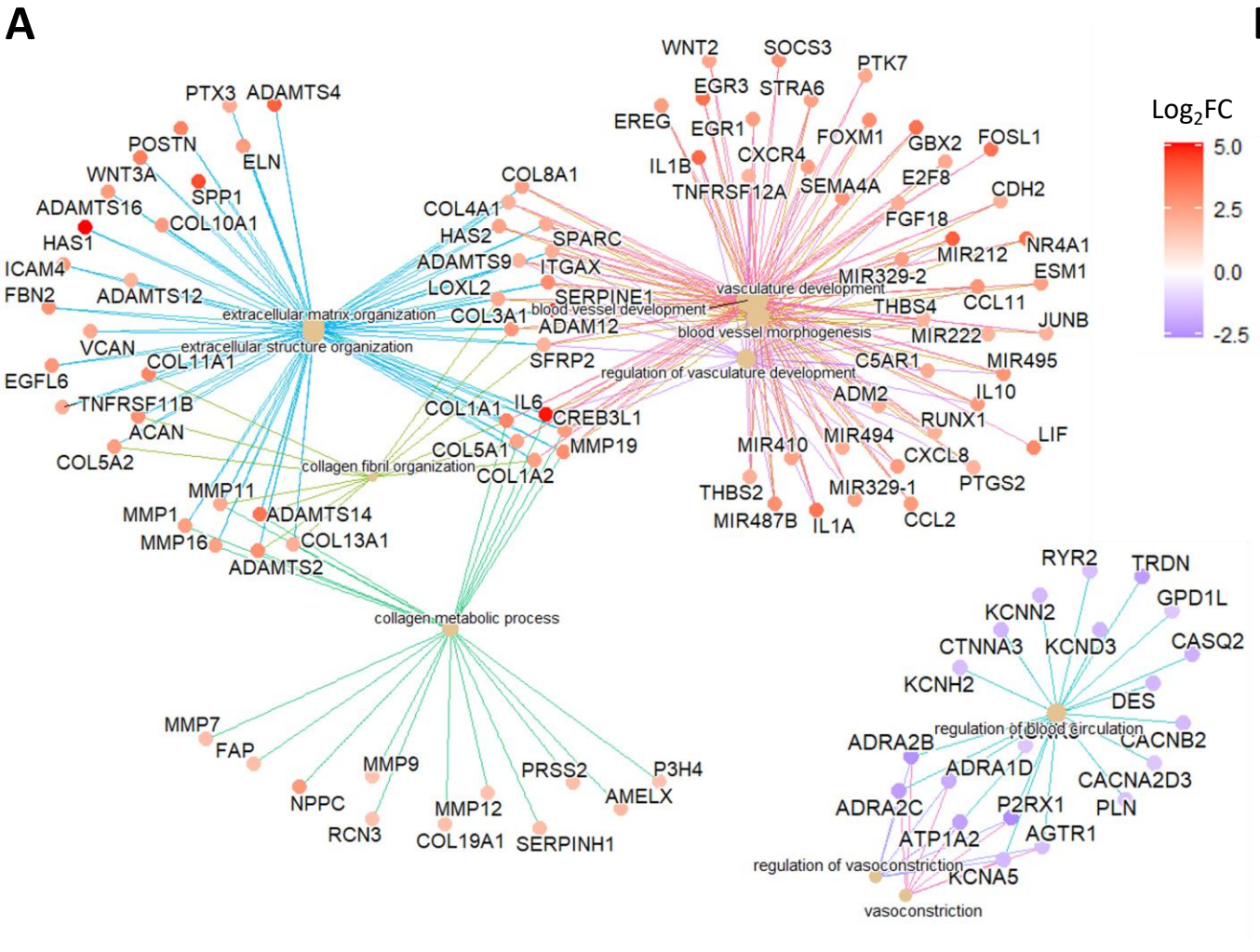

Supplementary Figure S2. Pathways involved in the vein to AVF transformation. A) Differentially expressed genes (absolute log2FC ≥ 1 in AVFs compared to veins; FDR<0.05) involved in activated and suppressed processes during the vein to AVF transformation. The color legend for gene nodes indicates the log2FC in AVFs compared to pre-access veins. **B)** Change in expression from the vein to the AVF in genes involved in suppressed pathways such as vasoconstriction and regulation of blood circulation (blue nodes in panel A). These include adrenergic receptors, potassium voltage-gated channels, and genes that participate in intracellular calcium signaling. Y-axes indicate normalized counts. FDR<0.05 for all paired comparisons.

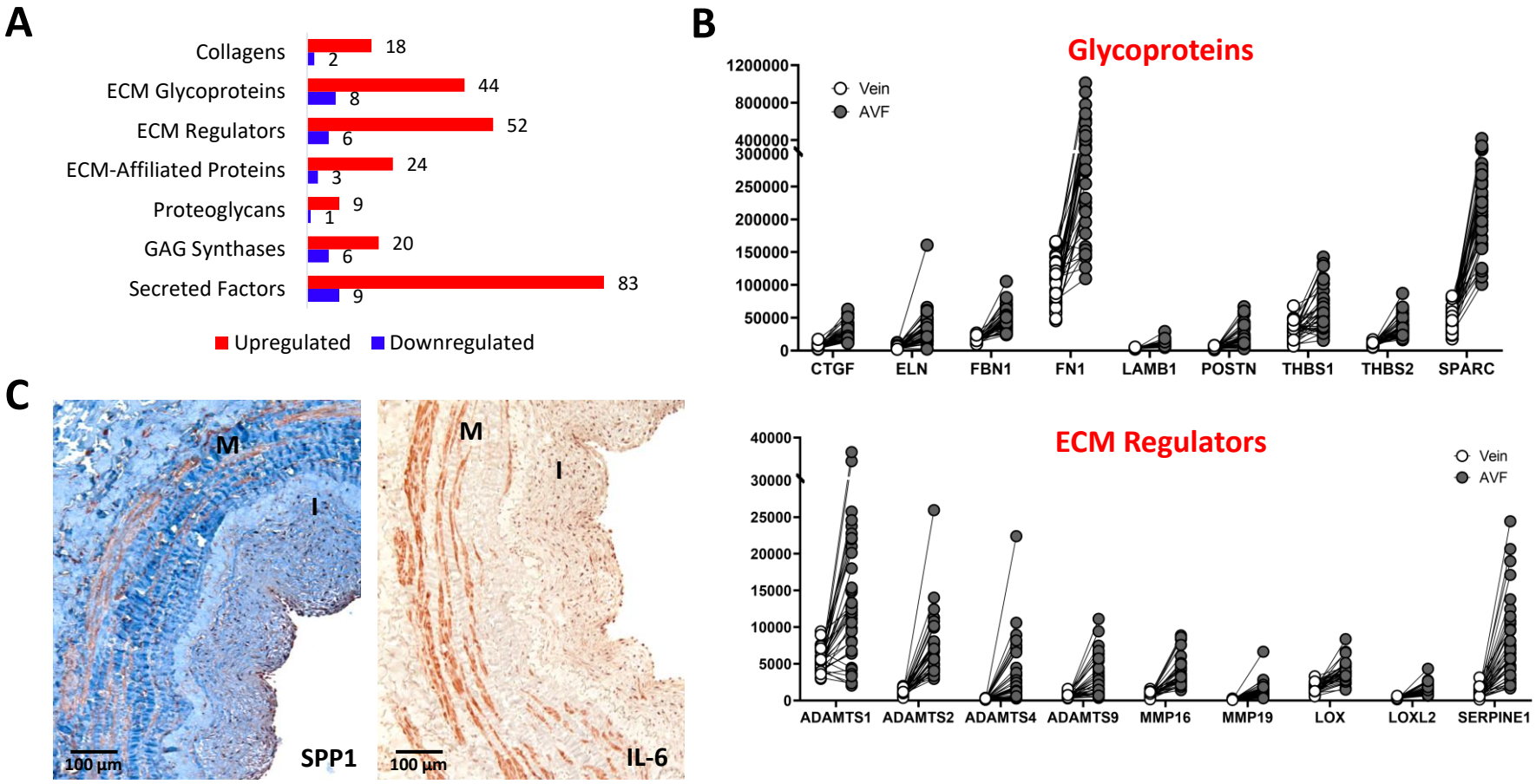

Supplementary Figure S3. Matrisome expression changes during the vein to AVF transformation. A) Distribution of differentially expressed matrisome genes (absolute log2FC ≥ 1 in AVFs compared to veins; FDR<0.05) by functional category and direction of expression changes. **B)** Examples of differentially expressed glycoproteins, extracellular matrix (ECM) regulators, and glycosaminoglycan (GAG) synthases. Y-axes indicate normalized counts. FDR<0.05 for all paired comparisons. **C)** Localization of osteopontin (SPP1) and IL-6 in the intima (I) and media (M) of AVFs by immunohistochemistry.

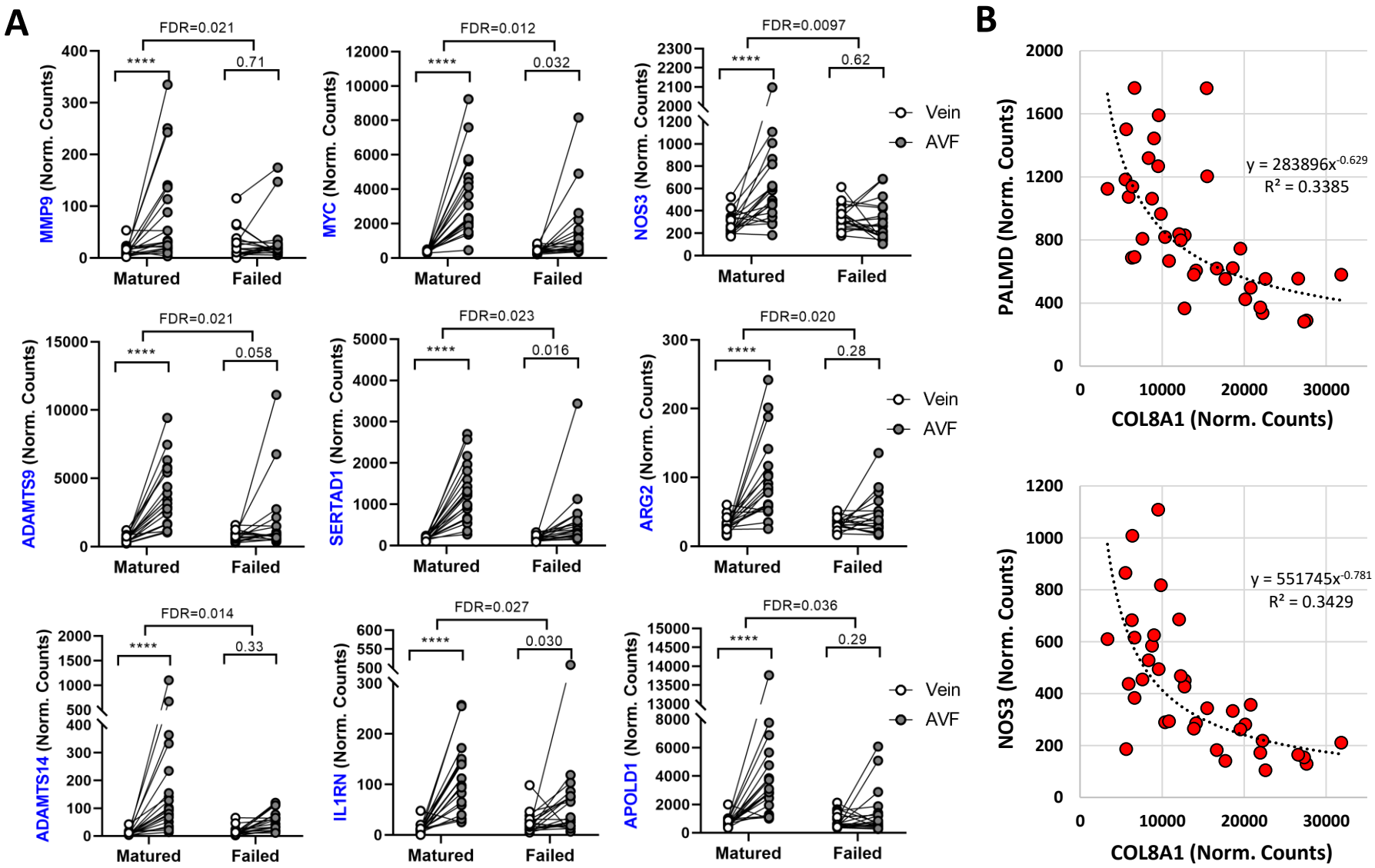

Supplementary Figure S4. Gene expression changes associated with AVF maturation failure. A) Examples of differentially expressed genes during the vein to AVF transformation in association with maturation failure. These include ECM regulators (MMP9, ADAMTS9, ADAMTS14), transcriptional regulators (MYC, SERTAD1), anti-inflammatory cytokines (IL1RN), and endothelial transcripts (NOS3, ARG2, APOLD1). Values above brackets indicate FDR for the corresponding comparison. ****FDR<0.001 **B)** Mathematical relationships between postoperative normalized counts of COL8A1 and those of PALMD and NOS3.

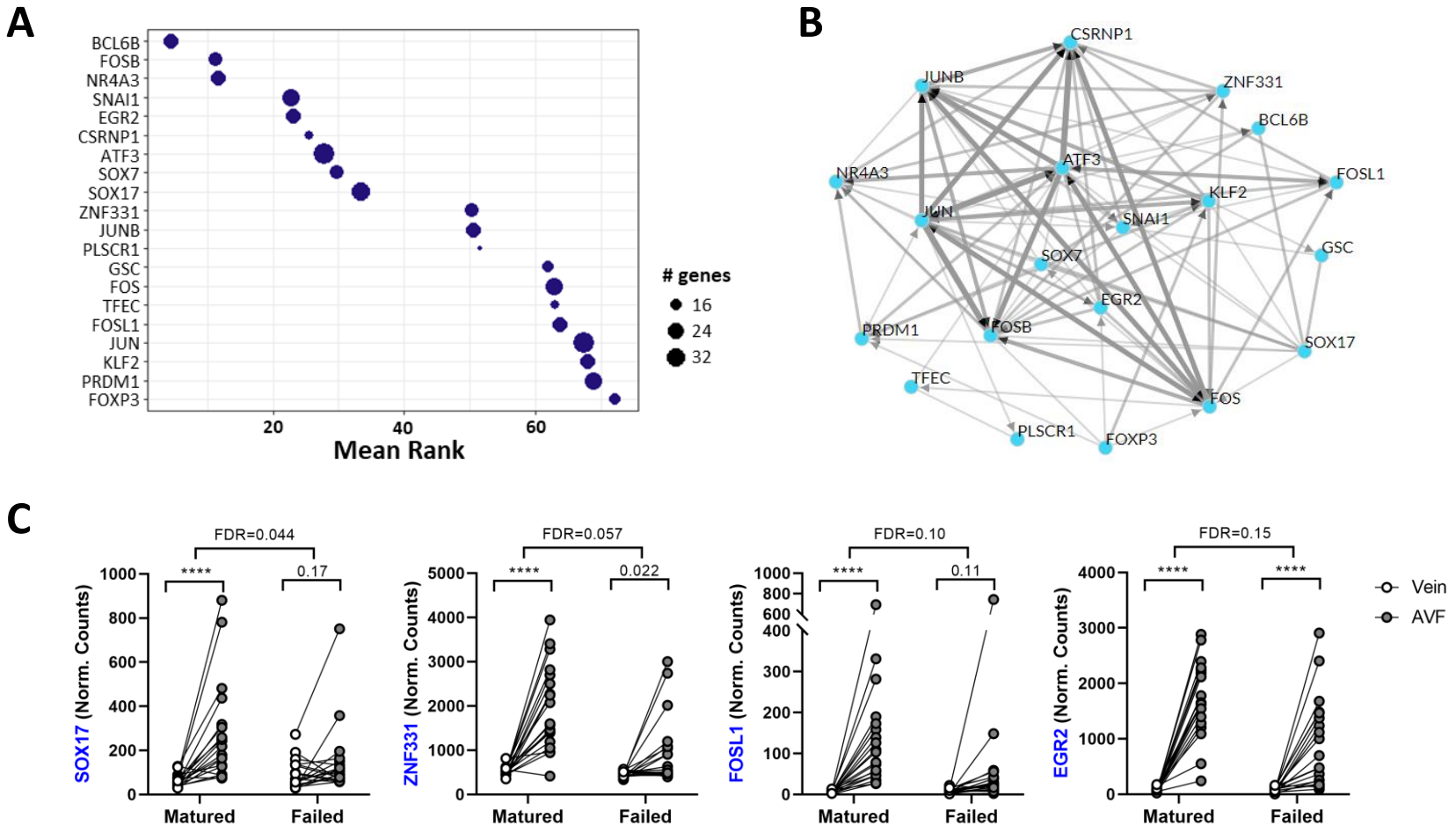

Supplementary Figure S5. Transcriptional regulation of genes associated with maturation failure. A) Transcription factor (TF) enrichment analysis indicating the 20 best ranked TFs in the transcriptional regulation of postoperative expression changes associated with maturation failure. This analysis ranks TFs based on the number of predicted targets in the input dataset (102 DEGs associated with failure) compared to the total number of targets experimentally identified by chromatin immunoprecipitation sequencing (ChIP-seq). For full list of TFs and putative target genes, refer to **Supplementary Data File S6. B)** Co-regulatory networks of factors in **A** indicating co-expression of TFs in ChIP-seq libraries (gray lines) or direct transcriptional regulation by an indicated factor (pointed arrows). **C)** Examples of differentially expressed TFs (SOX17, ZNF331) and TFs showing a statistical trend (FOSL1, EGR2) during the vein to AVF transformation in association with maturation failure. Values above brackets indicate FDR for the corresponding comparison. ****FDR<0.001